THE JOURNAL OF PHYSICAL CHEMISTRY B

Article

pubs.acs.org/JPCB

Effects of Temperature and Salt Addition on the Association Behavior of Charged Amphiphilic Diblock Copolymers in Aqueous Solution

Solmaz Bayati,[†,§] Kaizheng Zhu,[†] Loan T. T. Trinh,[†] Anna-Lena Kjøniksen,[†,‡] and Bo Nyström*[,†]

[†]Department of Chemistry, University of Oslo, P.O. Box 1033, Blindern, N-0315 Oslo, Norway

[‡]Department of Pharmaceutics, School of Pharmacy, University of Oslo, P.O. Box 1068, Blindern, N-0316 Oslo, Norway

ABSTRACT: Effects of temperature on the association behavior in aqueous solutions of a series of charged thermoresponsive poly(*N*-isopropylacrylamide)-*block*-poly((3-acrylamidopropyl) trimethylammonium chloride) (abbreviated as PNIPAAM$_n$-*b*-PAMPTMA(+)$_{20}$) with different lengths of the PNIPAAM block (n = 24, 48, and 65) have been studied with the aid of turbidimetry, zeta sizer, and dynamic light scattering (DLS). The turbidity results show that the transition to high turbidity values is shifted to lower temperatures when the length of the PNIPAAM block increases. It was observed that the value of the cloud point (CP) dropped with increasing polymer concentration, enlarged length of the PNIPAAM block, and augmented salinity. It was found that the decay of the correlation function from DLS is bimodal at temperatures well below CP, where the fast mode represents the motion of the unimers and the slow mode the dynamics of micelles/intermicellar complexes. At higher temperatures, larger particles of the system grow at the expense of the smaller ones in the spirit of Ostwald ripening, and clusters with a narrow size distribution evolve at high temperatures. By adding salt (NaCl), enhanced aggregation occurs at elevated temperatures because of screening of Coulomb repulsions.

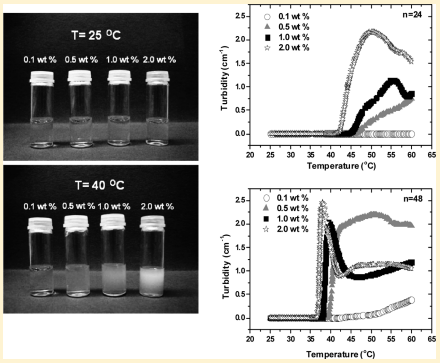

INTRODUCTION

In recent years, copolymers that can self-assemble in aqueous media have received great attention due to their ability to form nanostructured associated species like micelles or vesicles with a hydrophobic core and a hydrophilic shell.[1−10] Especially temperature-induced self-assembly of amphiphilic block copolymers has attracted considerable interest.[5,6,11−16] Poly(*N*-isopropylacrylamide) (PNIPAAM) is a typical example of a polymer that can act as a thermosensitive water-soluble block of the copolymer at low temperatures, whereas at temperatures above ca. 32 °C[17] (the lower critical solution temperature (LCST) of PNIPAAM) PNIPAAM collapses to form the core of the micellar structure. Typically, poly(ethylene glycol) (PEG) or methoxy-poly(ethylene glycol) (MPEG) is the hydrophilic block of the copolymer and it constitutes the corona that stabilizes the supramolecular structure. Polymeric micelles are attractive for drug delivery applications for targeting tissues and organs due to their nano-order sizes and the high loading capacity of hydrophobic drugs while maintaining their high stabilities in aqueous environment.[18]

The driving force for the molecular assembly of amphiphilic block copolymers in aqueous media is attributed to their differences in water solubility between hydrophobic and hydrophilic blocks. To illustrate this, let us consider a temperature-responsive diblock copolymer of the type[7] MPEG$_n$-*b*-NIPAAM$_m$, where the length of the NIPAAM block is constant and n is altered. In this case, temperature-induced association is promoted when the MPEG block is short ("crew-cut" micelles), whereas long MPEG chains ("hairy" micelles) reduce the tendency of the copolymer to form aggregates at elevated temperatures. Another way to improve the stability of particles is to attach a charged block to the copolymer to increase the stability of the species through repulsive electrostatic forces.[19]

In this work, we have synthesized a series of thermoresponsive poly(*N*-isopropylacrylamide)-*block*-poly((3-acrylamidopropyl)trimethylammonium chloride) diblock copolymers by utilizing atom transfer radical polymerization (ATRP).[20,21] The products obtained from this synthesis have the following composition: (PNIPAAM$_n$-*b*-PAMPTMA(+)$_{20}$). To explore the temperature-induced association features of this cationic diblock copolymer, three samples have been carefully designed and synthesized with the repeated units of NIPAAM blocks of n = 24, 48, and 65. This type of charged copolymer has previously been employed by our research group to investigate various phenomena in aqueous media such as normal and friction forces between silica surfaces[22] coated with adsorbed layers of the copolymer. Adsorbed onto gold particles at low surface coverage, this type of copolymer was found[23] to mediate flocculation of the particles at elevated temperatures. In a recent study,[24] a temperature-responsive inclusion complex of this type of copolymer and γ-cyclodextrin was reported. This

Received: July 10, 2012
Revised: August 14, 2012
Published: August 20, 2012

dx.doi.org/10.1021/jp306833x | *J. Phys. Chem. B* 2012, 116, 11386−11395

kind of temperature sensitive copolymer is known to form micelles in aqueous solution and quite recently the structure of these micelles was probed by using small X-ray scattering.[25]

The aim of this work is to gain a detailed insight into the intricate interplay between electrostatic stabilization of the micellar structures and temperature-induced association mediated by the PNIPAAM block. For this purpose, we have conducted turbidity, zeta-potential, dynamic light scattering measurements on different copolymer concentrations of PNIPAAM$_n$-*b*-PAMPTMA(+)$_{20}$ at various temperatures and different levels of salt (NaCl) addition. By changing the length of the PNIPAAM block, the idea is that the delicate interchange between electrostatic and associative interactions at elevated temperatures can be tuned by the length of the PNIPAAM block, and further modulation can be accomplished by adding salt. A deeper understanding of the intricate competition between associations and electrostatic interactions in systems of thermally sensitive charged copolymers is vital for the development of drug delivery systems.

EXPERIMENTAL SECTION

Materials, Synthesis, and Solution Preparation. Salt (NaCl) and all chemicals used for the synthesis of the copolymers were purchased from Aldrich and Fluka. The synthesis of the ligands (Me_6TREN), the purification of the monomers (NIPAAM and AMPTMA), and the initiator (ECP) followed the procedure described in the literature.[19,22,26] The copolymers have been synthesized by means of atom transfer radical polymerization (ATRP), which was carried out through a simple "one-pot" two-step ATRP procedure by using a water/*N*,*N*-dimethylformamide (DMF) = 50:50 (v/v) mixture as solvent at 25 °C. The initiator/catalyst system in the mixture contained ethyl 2-chloropropionate (ECP), CuCl, $CuCl_2$, and *N*,*N*,*N*′,*N*″,*N*‴,*N*‴-hexamethyltriethylenetetramine (Me_6TREN) (with molar feed ratio [ECP]/[CuCl]/[$CuCl_2$]/[Me_6TREN] = 1/1/0.6/1.6). The molar feed ratios of the two monomers [NIPAAM]/[AMPTMA] were 35/33, 55/33, and 75/33, corresponding to the diblock copolymers PNIPAAM$_n$-*b*-PAMPTMA(+)$_{20}$, with n = 24, 48, and 65, respectively. The preparation and purification procedures of the copolymers were conducted under similar conditions as described in detail previously.[19,22,25−27] The polymers were further purified by dialyzing against distilled water for several weeks using a dialysis membrane of regenerated cellulose with a molecular-weight cutoff of 3500. The white solid product was finally isolated by lyophilization. The synthesis route and structure of the copolymer are displayed in Figure 1.

In this work, analogues of the copolymer PNIPAAM$_n$-*b*-PAMPTMA(+)$_{20}$, with n = 24, 48, and 65, dissolved in aqueous solution have been investigated. All samples for turbidimetry, DLS, and zeta potential measurements have been prepared in the same way. For each sample, the proper amount of polymer, based on the desired concentration, was weighed and dissolved in distilled water at room temperature. The polymers were dissolved in water easily. The solutions were stirred for 24 h to ensure homogeneous solutions. Afterward, the samples were kept in a refrigerator for another 24 h and thereafter they were ready for measurements.

Characterization of the Copolymer. The chemical composition and structure of the charged synthesized diblock copolymers were ascertained by ^{1}H NMR using a Bruker AVANCE DPX 300 NMR spectrometer operating at 300.13 MHz at 25 °C by utilizing heavy water (D_2O) as the solvent.

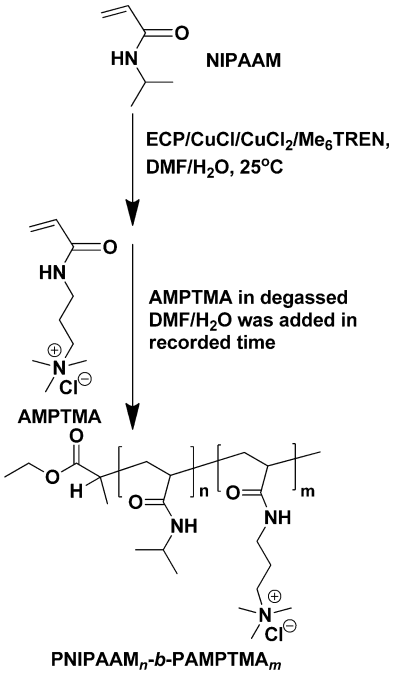

Figure 1. Chemical structure and synthesis route for the preparation of the PNIPAAM$_n$-*b*-PAMPTMA(+)$_{20}$ diblock copolymers via "one-pot" two-step ATRP.

The ^{1}H chemical shifts in D_2O are referred to the residual HDO proton (δ = 4.70 ppm) in D_2O. The repeat numbers of the NIPAAM and AMPTMA units were calculated from the integral values of the characteristic peak (peak 7 in Figure 2) of

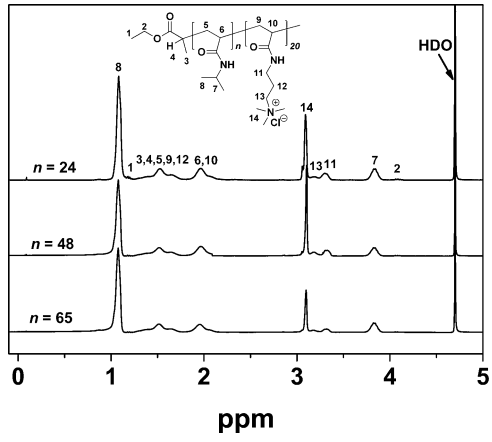

Figure 2. ^{1}H NMR spectra of the synthesized diblock copolymers PNIPAAM$_n$-*b*-PAMPTMA(+)$_{20}$ in D_2O (300 MHz).

PNIPAAM (δ = 3.82 ppm, N−C***H***$(CH_3)_2$, I_a), and of the methyl group of PAMPTMA (peak **14** in Figure 2) (δ = 3.10 ppm, −N(C***H***$_3)_3$, I_b) and the typical peak of the end group of the ethyloxyl group (peak **2** in Figure 2) (δ = 4.08 ppm, −OC***H***$_2$CH$_3$, I_c) based on the simple equation $n_{(NIPAAM)}$ = $2(I_a/I_c)$; $m_{(AMPTMA)}$ = $(2I_b/9I_c)$. Three diblock copolymers PNIPAAM$_n$-*b*-PAMPTMA(+)$_m$ with different repeating units of NIPAAM (n = 24, 48, and 65) and the same repeating units of AMPTMA (m = 20) have been successfully synthesized, by carefully adjusting the molar ratio of NIPAAM, AMPTMA, with the initiator ECP, as well as the polymerization time. The monomers/initiator (NIPAAM/AMPTMA/ECP) are 35/33/1,

dx.doi.org/10.1021/jp306833x | J. Phys. Chem. B 2012, 116, 11386−11395

55/33/1, and 75/33/1 for the samples with n = 24, 48, and 65, respectively. The compositions of the diblock copolymers are estimated to be n/m = 24/20, 48/20, and 65/20.

Asymmetric Flow Field-Flow Fractionation. The number average molecular weight (M_n), weight average molecular weight (M_w), and polydispersity indexes (M_w/M_n) were measured by asymmetric flow field-flow fractionation (AFFFF) for all considered block copolymers. The AFFFF experiments[6] were conducted on an AF2000 FOCUS system (Postnova Analytics, Landsberg, Germany) equipped with an RI detector (PN3140, Postnova) and a multiangle (seven detectors in the range 35−145°) light scattering detector (PN3070, λ = 635 nm, Postnova). The copolymer samples (2.0 wt % in 0.01 M NaCl) were measured using a 500 μm spacer, a regenerated cellulose membrane with a cutoff of 1000 (Z-MEM-AQU-425N, Postnova), and an injection volume of 20 μL. Although the concentration of the injected sample is rather high (2.0 wt %), it is strongly diluted in the course of the experiment and the results refer to a solution with a low concentration (the concentration of the sample passing through the detector is less than 0.03 wt %). To minimize aggregate formation, the measurements were carried out at 10 °C. Processing of the measured data was achieved by the Postnova software (AF2000 Control, version 1.1.025). Weight-average molecular weights of the samples in the dilute concentration regime were determined using this software with a Zimm-type fit, and a refractive index increment (dn/dc) of 0.156 (determined by using the RI detector at 32 °C). The characteristic data of the studied diblock copolymers are depicted in Figure 3. The results show that the copolymers have molecular weights between 6000 and 25 000 and the fractions have fairly narrow molecular weight distributions.

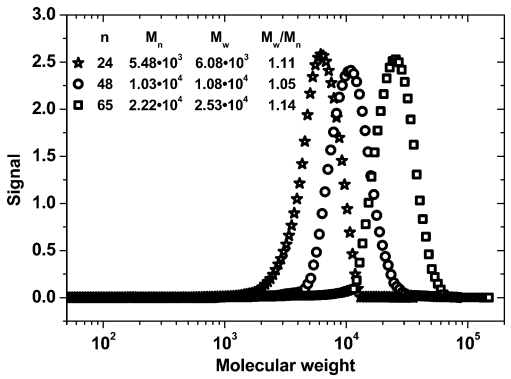

Figure 3. Illustration of the molecular weight distributions of the three PNIPAAM$_n$-*b*-PAMPTMA(+)$_{20}$ diblock copolymers in aqueous solutions (0.01 M NaCl) with the aid of AFFFF.

Zeta-Potential Experiments. The instrument that was employed in this study is a Zeta-sizer Nano ZS instrument, MAL1049741, made by Malvern instruments Ltd., United Kingdom. The sample cell that was used is a "dip" cell, including palladium electrodes with 2 mm spacing, one PCS1115 cuvette, and a cap. The experiments were carried out at a range of temperatures, and the equilibrium time at each temperature was ca. 1 min. The values of the electrophoretic mobility were converted to zeta potential values.

Turbidimetry. The instrument utilized in this work is a NK60-CPA cloud point analyzer made by Phase Technology, Richmond, BC, Canada. The light beam from a light source (AlGaAs, 654 nm) is focused on the sample by means of a lens. The 0.15 mL sample is injected by a micropipet on the specific glass plate, which is coated with a metallic layer with a very high reflective index. In fact, the plate works as a mirror. The temperature of the sample cell is controlled by a platinum resistance thermometer probe (Peltier elements). To avoid solvent evaporation during a temperature scan, each sample has been covered by the same amount of silicon oil. The scattered intensity signal (S) is detected by the light scattering detector, which is located directly above the investigated sample. The turbidity (τ) and the scattered intensity signal are related to each other by the empirical equation[3] $\tau = 9.0 \times 10^{-9}\ S^{3.751}$. The heating rate in each measurement is 0.2 °C/min over the temperature range 25−60 °C. Lower heating rates were not possible due to instrumental limitations. However, the effect of heating rate on the signal is not expected to be significant at low heating rates. The temperature at which the first deviation of the scattered intensity from the baseline occurred was taken as the cloud point (CP) of the considered sample.

Dynamic Light Scattering. Dynamic light scattering (DLS) experiments were carried out by means of an ALV/CGS-8F multidetector version compact goniometer system, with eight fiber-optical detection units, from ALV-GmbH., Langen, Germany. Further experimental details of this equipment can be found in a previous work.[19]

The DLS experiments were performed with a temperature gradient of 0.05 °C/min. The correlation function data were recorded continuously with an accumulation time of 1 min. The intensity correlation function was measured at eight scattering angles simultaneously in the range 22−141° with 4 ALV5000/E multiple-τ digital correlators. The temperature in the measuring cell is controlled to within ±0.01 °C with a heating/cooling circulator. The copolymer solutions were filtered in an atmosphere of filtered air through a 5 μm filter (Millipore) directly into precleaned NMR tubes. In the temperature range considered in this work, no problems with multiple scattering effects were encountered.

In the solutions of these copolymers, the experimentally recorded intensity autocorrelation function $g^2(q,t)$ is directly related to the theoretically amenable first-order electric field autocorrelation function $g^1(q,t)$ through the Siegert[28] relationship $g^2(q,t) = 1 + B|g^1(q,t)|^2$, where B ($\leq$1) is an instrumental parameter and $q = (4\pi n/\lambda)\sin(\theta/2)$, where λ, θ, and n are the wavelength of the incident light in a vacuum, scattering angle, and refractive index of the medium, respectively.

At temperatures below CP, the correlation functions can be described accurately by the sum of a single exponential and a stretched exponential function as follows

$$g^1(t) = A_f \exp[-t/\tau_f] + A_s \exp[-(t/\tau_{se})^{\beta}] \quad (1)$$

with $A_f + A_s = 1$. The parameters A_f and A_s are the amplitudes for the fast and slow relaxation modes, respectively. The stretched exponent β characterizes the width of the distribution of relaxation times. The variables τ_f and τ_{se} are the relaxation times characterizing the fast and the slow relaxation process, respectively. At higher temperatures, when most of the unimers have been consumed in the formation of intermicellar structures and the fraction of large species dominates, the correlation functions could be fitted with a single stretched exponential ($g^1(t) = \exp[-(t/\tau_{se})^{\beta}]$).

Bimodal relaxation processes have recently been reported[3,13,29,30] from DLS studies on associating polymer systems of various natures. In the analysis of the correlation

dx.doi.org/10.1021/jp306833x | J. Phys. Chem. B 2012, 116, 11386−11395

functions with the aid of eq 1, a nonlinear fitting algorithm was employed to obtain best-fit values of the variables A_f, τ_f, τ_{se}, and β appearing on the right-hand side of eq 1. The fast relaxation time yields the mutual diffusion coefficient D ($\tau_f^{-1} = Dq^2$) of unimers, and τ_{se} characterizes the dynamics of large clusters or intermicellar structures. Through the stretched exponent ($0 < \beta \leq 1$), the mean relaxation time for the slow mode is given by

$$\tau_s = \frac{\tau_{se}}{\beta}\Gamma\left(\frac{1}{\beta}\right) \tag{1a}$$

where Γ is the gamma function. From the relaxation modes, we are able to determine the apparent hydrodynamic radii ($R_{h,f}$ and $R_{h,s}$) from the fast and slow relaxation times, respectively, via the Stokes–Einstein relation $R_h = k_BT/6\pi\eta_0 D$, where k_B is the Boltzmann constant, T is the temperature, η_0 is the solvent viscosity, and D is the mutual diffusion coefficient of unimers or micelles/intermicellar complexes. We should note that the Stokes–Einstein relation is strictly valid only in the absence of interparticle interactions and internal motions, that is, $qR_h < 1$. For some very large species considered in this study, this criterion is not fulfilled and some corrections to R_h should be made to obtain accurate values of R_h. However, since we are more concerned with the characteristic growth of clusters with increasing temperature, rather than the real cluster size itself, this correction is not crucial.

RESULTS AND DISCUSSION

In aqueous solutions of amphiphilic copolymers, the micellization process is controlled by the critical micelle concentration and the critical micelle temperature, and at higher polymer concentration and/or elevated temperatures, intermicellar structures are formed.[5,31] In this investigation, effects of polymer concentration, temperature, and salt addition on the formation of intermicellar complexes in solutions of a charged diblock copolymer with different lengths of the NIPAAM block will be analyzed by using zeta-sizer, turbidity, and dynamic light scattering.

Zeta Potential Measurements. Figure 4 clearly shows that all diblock copolymers are positively charged, as expected, and the charge density increases as the temperature rises. This type of behavior has previously been reported[32] for charged copolymers, and it is attributed to shrinking of the micelle-like clusters at elevated temperatures; therfore, the charged ammonium groups are forced out to the surfaces of the copolymer moieties. This effect is more pronounced for the longer PNIPAAM blocks because the contraction of the species should be more accentuated when the number of hydrophobic segments in the core is augmented. The hypothesis is that enhanced charge density will stabilize the particles and counteract the tendency of forming association complexes at higher temperatures. It has earlier been shown[19] that charges can prevent growth of intermicellar structures.

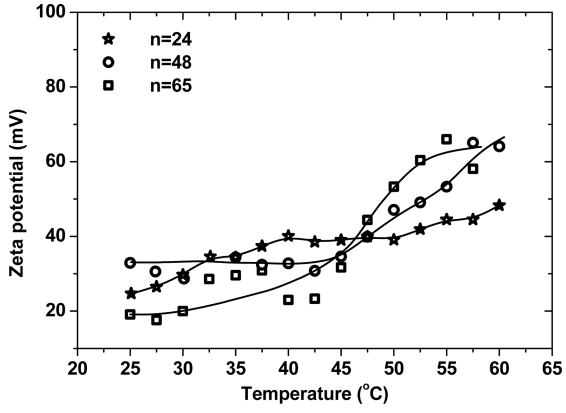

Figure 4. Plot of the zeta potential versus temperature for 0.05 wt % solutions of all diblock copolymers.

Turbidimetry. Turbidimetry is a powerful method to reveal association behavior on a mesoscopic scale for solutions that exhibit, e.g., a lower critical solution temperature. The picture in Figure 5 for solutions of the diblock copolymer (n = 48) shows that no cloudiness can be observed for any of the solutions at 25 °C, whereas at 40 °C the solutions become gradually more cloudy as the polymer concentration increases. This demonstrates that large association complexes are formed at higher concentrations. At the lowest polymer concentration of the copolymer with the shortest PNIPAAM block (n = 24), virtually no change of the turbidity is detected in the considered temperature region. However, a closer inspection of the turbidity curve reveals an incipient turbidity increase at elevated temperatures, making it possible to estimate a cloud point also for this sample. As the concentration increases, a progressively stronger temperature dependence of the turbidity evolves and the transition occurs at lower temperatures. It is obvious that a higher polymer concentration promotes the evolution of large intermicellar structures at elevated temperatures even when the species are decorated with charge.

For the diblock copolymer with a longer PNIPAAM block (n = 48), a temperature-induced turbidity rise is observed even at the lowest concentration, and at higher concentrations, a transition peak in the turbidity is observed. This type of behavior has been reported[6,7,10,19,26] in the past for solutions of amphiphilic copolymers; this effect was ascribed to a perpetual competition between the growth of the intermicellar clusters and the compression of the species.

Figure 6 illustrates the effects of polymer concentration, length of the PNIPAAM block, and salt addition on the cloud point for solutions of the considered diblock copolymers. For the three diblock copolymers with different lengths of the PNIPAAM block, it is clear that the value of CP decreases as the polymer concentration rises (Figure 6a); this tendency is strongest for the copolymer with the shortest PNIPAAM block. This tendency parallels the behavior observed[26] in aqueous solutions of PNIPAAM of different molecular weights. It was argued that the concentration dependence of CP is less pronounced as the molecular weight of the sample is increased because the influence of molecular weight on the value of CP diminishes at sufficiently high molecular weights. At higher molecular weights, the concentration-induced depression effect of the cloud point is less pronounced, because the number of hydrophobic segments plays a less dominant role for the formation of aggregates for long polymer chains. The drop of the cloud point with increasing polymer concentration seems to be a general feature for copolymers containing PNIPAAM. For instance, in a recent study[33] on aqueous solutions of thermoresponsive poly(ethylene glycol)-*block*-poly(*N*-isopropylacrylamide)-*block*-poly(ε-caprolactone) (PEG_{43}-*b*-$PNIPAAM_{82}$-*b*-PCL_{87}) triblock copolymer, the value of CP decreases significantly with increasing polymer concentration.

The turbidity and cloud point behavior may be rationalized in the following scenario. As the temperature rises, the moieties become gradually more "sticky" and higher concentration

dx.doi.org/10.1021/jp306833x | J. Phys. Chem. B 2012, 116, 11386–11395

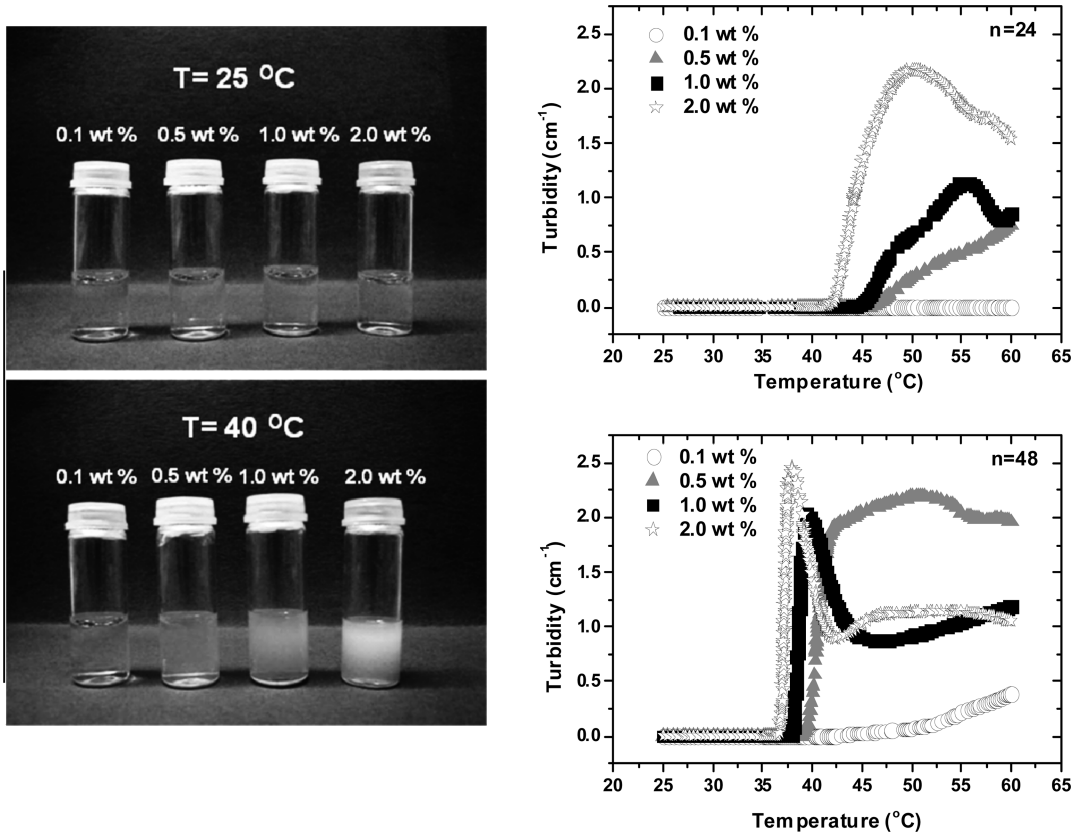

Figure 5. Picture illustrating the visual cloudiness upon a temperature rise (n = 48) and the temperature dependences of the turbidity at a heating rate of 0.2 °C/min for the diblock copolymers with n = 24 and n = 48 at the polymer concentrations indicated.

favors higher collision frequency of the species and this leads to enhanced turbidity. The depression of CP with increasing polymer concentration may be interpreted in terms of the effective Flory–Huggins interaction parameter χ_{eff},[34,35] where χ_{eff} is a function of both temperature (T) and concentration (c), $\chi_{eff}(T,c)$. At a given temperature, the rise of χ_{eff} as the polymer concentration increases is attributed to poorer solvent conditions, or association of self-assembled moieties. The impacts of concentration and temperature on the formation of aggregates in polymer solutions have been addressed in several theoretical approaches.[36−39] One special model was elaborated by de Gennes[37] for the interpretation of the association behavior in aqueous poly(ethylene oxide) solutions. In this approach, the concentration dependence of χ_{eff} is related to attractive interactions leading to stable clusters of $n > 2$ monomers (e.g., micelles), while monomer–monomer interactions remain repulsive. This is a type of two-state model for associating polymers, where a dynamic equilibrium between "clustered" and "non-clustered" monomers exists. This model predicts a situation at poor solvent conditions, where a dilute solution of single polymer species coexists with a dense polymer phase (e.g., aggregates). In the approach elaborated by Painter,[38] the concentration dependence of χ_{eff} is described in terms of the interplay between intrachain and interchain contacts. In general, it can be argued from these models that the observed decrease of CP with increasing polymer concentration can be ascribed to more intensive intermolecular associations at higher concentrations, leading to a reduction of the cloud point temperature.

Since the PNIPAAM block in the diblock copolymers is expected to be crucial for the turbidity features of the copolymers, it is interesting to make a comparison of the CP values with solutions of the PNIPAAM homopolymer with the same chain lengths as PNIPAAM blocks of the copolymers considered in this study. Let us consider 1 wt % solutions of PNIPAAM$_n$-*b*-PAMPTMA(+)$_{20}$ with n = 48 and n = 65. In this case, the values of the cloud point are 37.6 °C for n = 48 and 36.0 °C for n = 65, whereas, for the PNIPAAM homopolymer[26] with approximately the same chain lengths as the corresponding diblock copolymers, the values of CP are 36.9 and 32.2 °C, respectively. The higher CP values for the diblock copolymers as compared with the analogous homopolymers can be ascribed to improved stability of the species because of the charges onto the copolymer species. However, at higher temperatures, the charged copolymers also form large intermicellar structures, as indicated by high turbidity values. It is generally claimed that PNIPAAM becomes more hydrophobic at temperatures above the lower critical solution temperature, but in a recent paper,[40] it was argued PNIPAAM is not a hydrophobic material at temperatures above the LCST. It was stated that the isopropyl groups and the polymethylene backbones are hydrophobic both above and below the LCST. Temperature dependent solute interactions occur when solute–isopropyl group interactions are energetically more favorable for isopropyl groups in a polymer rich environment compared to isopropyl groups in water or *vice versa*. The general idea from the cited investigation is that temperature-induced interactions between PNIPAAM and solutes arise because of changes in the local environment around the hydrophobic isopropyl domains. Below the LCST, the isopropyl groups are surrounded by water, whereas above the LCST the hydrophobic groups are in contact with both water and polymer segments. In a similar way, PNIPAAM is

dx.doi.org/10.1021/jp306833x | J. Phys. Chem. B 2012, 116, 11386−11395

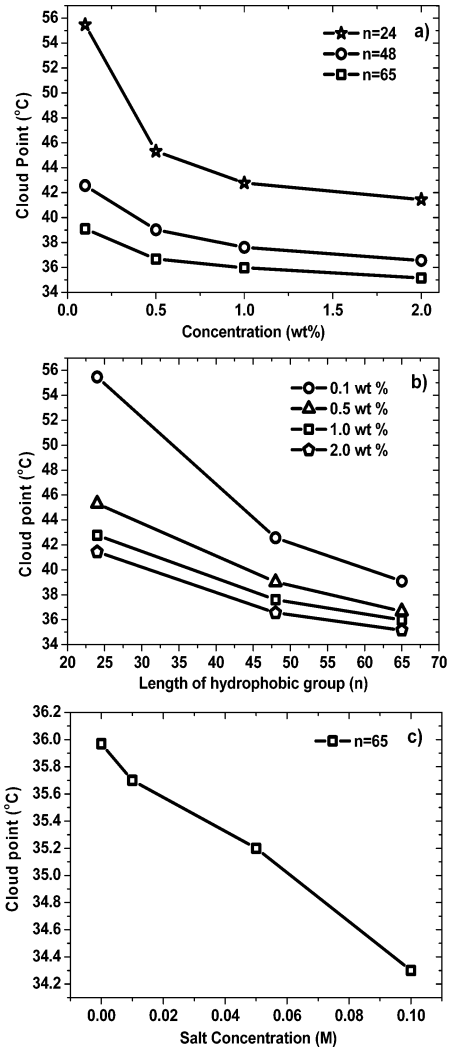

Figure 6. Effects of polymer concentration (a) and length of the PNIPAAM block (b) on the cloud point for aqueous solutions of the three diblock copolymers. (c) Effect of salt addition (NaCl) on the cloud point for 1 wt % solution of $PNIPAAM_{65}$-*b*-$PAMPTMA(+)_{20}$.

not completely hydrophilic because it has hydrophilic and hydrophobic domains above and below the LCST. By using molecular dynamics simulations on aqueous PNIPAAM solutions, the results from a recent study[41] on a multiple-chain system indicate that collective interactions are a necessary requirement to observe the LCST.

Figure 6b shows that an increase in the length of the PNIPAAM block leads to a depression of the CP at all studied polymer concentrations, but this trend is more prominent at a low concentration because of the lower collision frequency the "sticking" probability will be more sensitive for a long PNIPAAM block. These results clearly disclose that, even for block copolymers with high charge density, the length of the PNIPAAM block is vital for the formation of the intermicellar complexes and the cloudiness of the solutions at elevated temperatures.

To gain more insight into the importance of the electrostatic interactions, the effect of salt addition on the cloud point for 1 wt % solutions of $PNIPAAM_{68}$-*b*-$PAMPTMA(+)_{20}$ is depicted in Figure 6c. By adding salt, the electrostatic interactions are gradually screened. It is obvious that the cloud point is depressed upon salt addition; this demonstrates that weaker repulsive electrostatic interactions promote aggregation and shift the cloud point toward lower temperatures. The results from this study clearly reveal that the electrostatic stabilizing effect of the particles is strongly counteracted by the interchain associations generated through PNIPAAM segments at high temperatures.

Dynamic Light Scattering. The light scattering data were recorded continuously at a heating rate of 0.05 °C/min. Normalized correlation functions at a scattering angle of 107° for 1 wt % solutions of $PNIPAAM_n$-*b*-$PAMPTMA(+)_{20}$ are displayed in Figure 7 in the form of semilogarithmic plots. Each

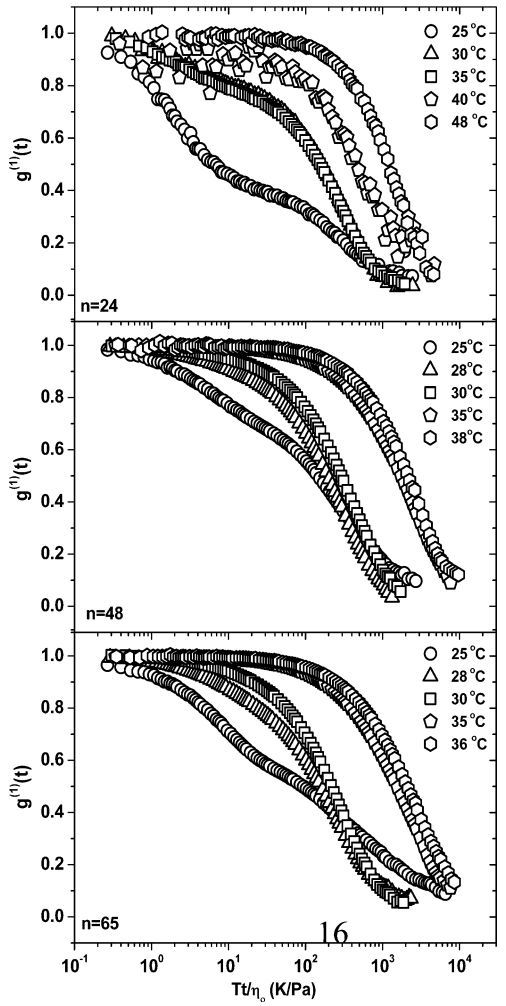

Figure 7. Plot of the first-order electric field autocorrelation function $g^{(1)}(t)$ versus tT/η_o at a scattering angle of 107° for all three copolymers at a concentration of 1 wt %.

measurement took ca. 1 min, and the temperature refers to the mean temperature during an experiment. In this work, very slow heating rates were utilized to avoid significant temperature-induced changes during accumulation of the correlation functions. To take into account trivial changes of the solvent viscosity (η_0) with temperature (T), the correlation function data have been plotted against tT/η_0. The general trend for all copolymers is that the tail of the correlation function is shifted toward longer times as the clusters grow at elevated temperatures. An inspection of the correlation functions reveals at low temperatures a bimodal appearance, which can initially be described by a single exponential, followed at longer times

dx.doi.org/10.1021/jp306833x | J. Phys. Chem. B 2012, 116, 11386−11395

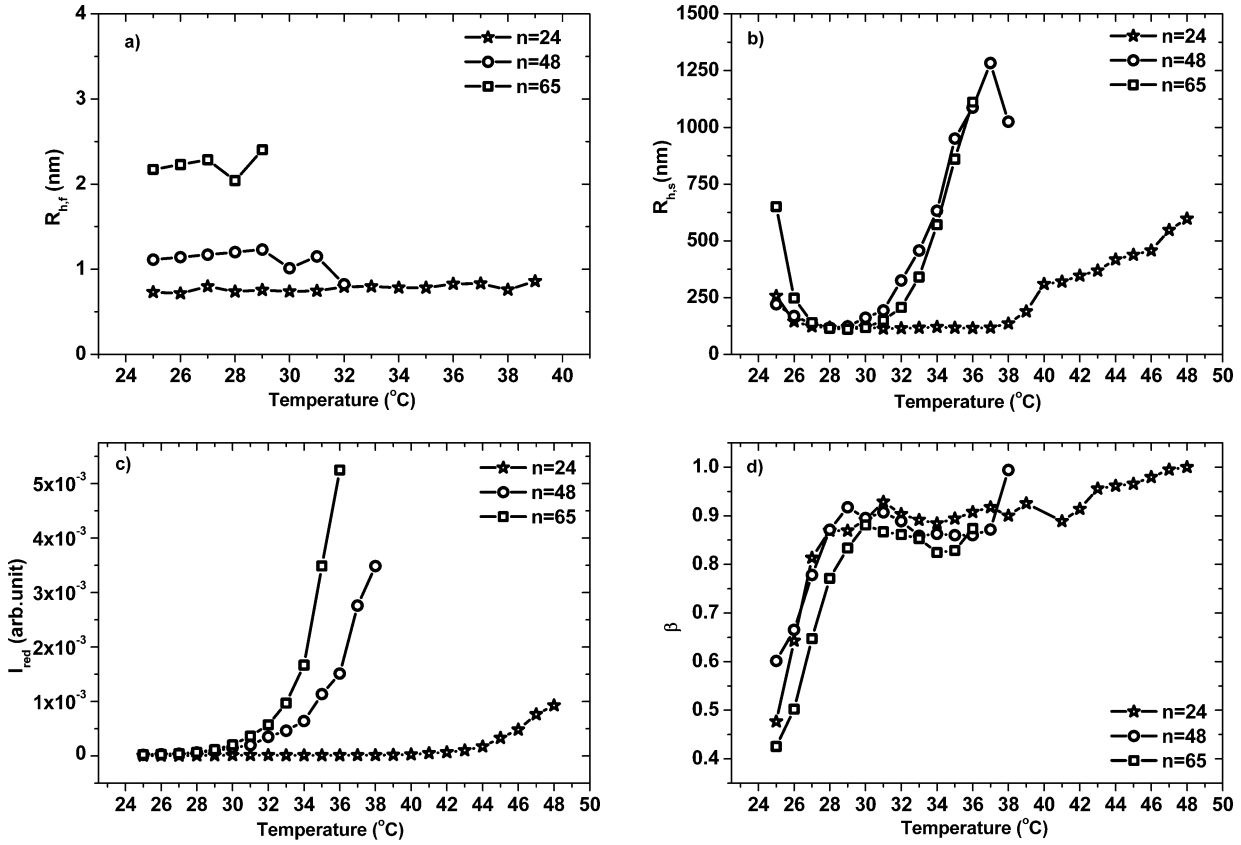

Figure 8. (a, b) Temperature dependencies of the apparent hydrodynamic radii determined from the fast relaxation time ($R_{h,f}$) and the slow relaxation time ($R_{h,s}$) through the Stokes−Einstein relationship for 1 wt % solutions of PNIPAAM$_n$-*b*-PAMPTMA(+)$_{20}$. (c) The reduced scattered intensity versus temperature for 1 wt % solutions of the copolymers. (d) The temperature dependence of the stretched exponent for the copolymers at 1 wt % solutions.

by a stretched exponential (see eq 1). At high temperatures, the fast mode fades away and the decay of the correlation can be portrayed by a single stretched exponential. This is because the size and number of the formed aggregates increase and the impact of the small entities (unimers) is strongly reduced, and it is not possible to extract the fast relaxation mode (cf. the discussion below).

Figure 8a,b shows the temperature dependences of the apparent hydrodynamic radii, corresponding to the fast mode ($R_{h,f}$) and the slow mode ($R_{h,f}$) for 1 wt % solutions of PNIPAAM$_n$-*b*-PAMPTMA(+)$_{20}$ with n = 24, 48, and 65. The rather limited temperature range covered by $R_{h,f}$ is because of the low fraction of single molecules at higher temperatures and the dominance of the large clusters. Since interchain association is strengthened as the length of the PNIPAAM block increases, the temperature region at which the fast relaxation mode can be detected is reduced when the value of n is raised. The small values of $R_{h,f}$ suggest that the sizes of unimers or single molecules are probed by the fast mode. As expected, the size of the entities increases with increasing length of the PNIPAAM block and virtually no temperature dependence is observed for the copolymer with n = 24. In the case of the copolymers with longer PNIPAAM block, a minute shrinking can be traced but the effect is very small. In a recent study[42] on single-molecule behavior of thermoresponsive copolymers containing PNIPAAM, Monte Carlo simulations showed a temperature-induced compression of the single copolymer molecules and the magnitude of this effect was found to be larger as the length of the PNIPAAM block increased.

The slow mode probes the relaxation of micelles and intermicellar structures, and their sizes are given by $R_{h,s}$ (Figure 8b). The general trend is the compression of the species that occurs well below the CP of the system, followed by the growth of the interchain complexes at higher temperatures. The initial drop of $R_{h,s}$ is more marked as the length of the PNIPAAM block is increased because larger interchain complexes are formed with more PNIPAAM chains that can facilitate the contraction of the species. At higher temperature, the interchain aggregation prevails and huge complexes are gradually formed. At still higher temperatures, multiple scattering obstructs analyses of the correlation functions. The start and the intensity of the growth process are governed by the length of the PNIPAAM block. It should be noted that the initial growth of the complexes commences at temperatures well below the cloud point of the samples (cf. Figure 6). Even for these highly charged copolymers, the findings divulge that the intensity of the aggregation behavior is significantly affected by the length of the PNIPAAM block. For the copolymer with the shortest PNIPAAM block (n = 24), the incipient growth of the species occurs at much higher temperature than for copolymers with longer PNIPAAM blocks. Actually, a similar trend has been reported[26] for PNIPAAM homopolymers. The small divergence in behavior observed for the copolymers with n = 48 and n = 65 can be ascribed to the small difference in PNIPAAM block size between the two polymers.

The difference in behavior between the copolymer samples is further accentuated by the reduced scattered intensity results on 1 wt % solutions of the diblock copolymers (see Figure 8c).

dx.doi.org/10.1021/jp306833x | *J. Phys. Chem. B* 2012, 116, 11386−11395

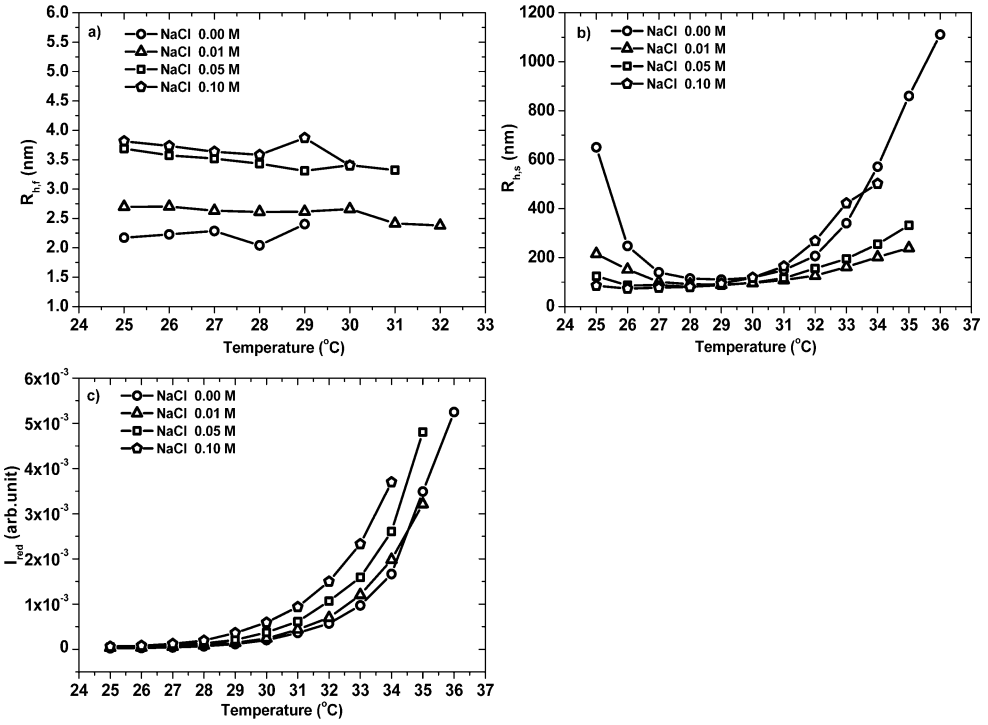

Figure 9. Temperature dependences of $R_{h,f}$ (a), $R_{h,s}$ (b), and the reduced scattered intensity (c) for 1 wt % solutions of PNIPAAM$_{65}$-*b*-PAMPTMA(+)$_{20}$ at a scattering angle of 107° and at the levels of salt addition indicated.

It is clear that the reduced scattered intensity starts to rise at lower temperatures when the length of the PNIPAAM is increased. The difference in temperature dependence of the reduced scattered intensity for the samples with n = 48 and n = 65 is more pronounced than for the corresponding effect in $R_{h,s}$. In this case, the increase in the scattered intensity can be caused both by the formation of large clusters and by the compression of the clusters.[43,44] This suggests that, even though the sizes of the aggregates formed at elevated temperatures for the n = 48 and n = 65 samples are similar, the contraction effect is expected to be more marked for the n = 65 sample. The similarity in sizes is therefore likely because of the stronger contracted structure of the association complexes formed by the polymer with the longest PNIPAAM block in combination with a higher close-packing of the chains. Again, the size of the PNIPAAM block is shown to be crucial for the temperature-induced growth of the complexes.

In the interpretation of the findings reported above, it may be instructive to consider Ostwald ripening[45] as a framework for the cluster growth process. Ostwald ripening, or coarsening, of a precipitate is the final stage of a macroscopic phase separation in a solution, during which larger particles of the precipitate grow at the expense of the smaller ones owing to the higher solubility of the smaller particles (Gibbs−Thomson or Kelvin effect) and the molecular diffusion through the continuous phase. In this process, the small entities will gradually disappear. A theoretical description of Ostwald ripening in two-phase systems was originally elaborated independently by Lifshitz and Slyozov[46] and by Wagner[47] (LSW theory). Some of the main assumptions for this model are as follows: (i) Molecular diffusion is the rate-determining step for the transport of material between the particles. (ii) There are no particle interactions; i.e., the system is very dilute. (iii) The particles are spherical and fixed in space. After the development of this pioneering model, a more detailed theoretical understanding of this phenomenon has emerged (cf. the review article by Voorhees[48]). It has been argued from theoretical models,[47−49] based on the LSW theory, and simulation studies[49−51] that Ostwald ripening can result in narrow size distributions. A previous theoretical study[52] suggests that diffusion-controlled aggregation of particles promotes narrow size distributions. The prediction of narrow size distributions of the clusters in the framework of Ostwald ripening collaborates well with the results in Figure 8d. In the analyses of the correlation function data, a stretched exponential function was utilized and the temperature dependence of the stretched exponent β is depicted in Figure 8d. It is evident that β approaches 1 as large complexes are formed and the unimers disappear. This feature signals that the size distribution is very narrow.

To examine the impact of charged groups on the association features of the copolymers, various amounts of NaCl were added to the PNIPAAM$_{65}$-*b*-PAMTMA(+)$_{20}$ sample. By increasing the salt concentration, the electrostatic interactions in the systems are gradually screened and this may improve our understanding about the influence of electrostatic interactions in these systems. Figure 9a,b shows the temperature dependences of the apparent hydrodynamic radii $R_{h,f}$ and $R_{h,s}$, extracted from the fast and slow relaxation modes, respectively. The apparent hydrodynamic radius $R_{h,f}$ exhibits only a slight decrease with increasing temperature, and this is probably due to dense-packing of the hydrophobic segments at higher temperature. The general trend is that the size of the moieties increases as the salinity increases, and this is ascribed to the screening of electrostatic repulsion resulting in a higher aggregation number. This finding has been reported[10,53] for other charged copolymers upon addition of salt. It should be mentioned that similar effects have also been found[54] for homopolymer polyelectrolytes.

The temperature dependence of $R_{h,s}$, calculated from the slow relaxation time, displays a different behavior than $R_{h,f}$

dx.doi.org/10.1021/jp306833x | J. Phys. Chem. B 2012, 116, 11386−11395

when salt is added. In this case, we have large intermicellar structures that are strongly influenced by temperature. Initially, at low temperatures, $R_{h,s}$ drops when the level of salt addition increases and this is attributed to screening of the electrostatic repulsion as the salinity rises. The initial temperature-induced compaction of the clusters is less pronounced as the salinity rises, because at low salinity or without salt the intermicellar structures are expanded through electrostatic repulsive forces and as the cloud point is approached the dense-packing of the hydrophobic segments will generate a strong compaction of the complexes.

At high temperatures, an intriguing temperature dependence emerges for $R_{h,s}$, where a marked increase of $R_{h,s}$ is observed for the copolymer without added salt. This shows the strong growth of the intermicellar complexes at high temperatures; this trend is compatible with the pronounced rise of the reduced scattered intensity at elevated temperatures (see Figure 9c). However, at a low level of salt addition, only a moderate increase of $R_{h,s}$ is observed and this finding indicates that a stabilization of the clusters occurs at a low salt concentration. At the highest level of salt addition (0.1 M), intermicellar fusion generates large complexes due to screening of the electrostatic interactions. The reason for the special behavior at intermediate salt concentrations is not clear, but it is known[53,55] that the effect of salt addition in solutions of aggregated polyelectrolytes is more complex than that in solutions of free polyelectrolytes because of strong interchain interactions and the phenomenon of counterion condensation in micelles. It has been argued[56,57] that low salinity may suppress intermicellar fusion. It seems that the intricate interplay between Coulomb repulsion and counterion activity stabilizes the micellar structure at low salt concentration. It should be mentioned that the profiles of the correlation functions are similar to those in salt-free solutions, and high values of β at high temperatures are also observed in solutions with salt.

CONCLUSIONS

In this work, some novel features in aqueous solutions of a thermoresponsive cationic diblock copolymer (PNIPAAM$_n$-*b*-PAMPTMA(+)$_{20}$) with different lengths of the PNIPAAM block are reported. The main findings from this study can be summarized in the following way: (i) The charge density increases significantly with increasing temperature for all three copolymers, and this feature suggests that the charges are pressed out onto the surface of the particles and this observation indicates that the charged groups constitute the shell and PNIPAAM the core when the core−shell particles are formed. (ii) The magnitude of the temperature-induced turbidity change becomes larger as the length of the PNIPAAM block is enlarged and as the polymer concentration increases. It is observed that the value of the cloud point drops with increasing polymer concentration, enlarged length of the PNIPAAM block, and augmented salinity. (iii) The decay of the correlation function from DLS is bimodal at temperatures well below CP, where the fast mode represents the motion of the unimers and the slow mode the dynamics of micelles/intermicellar complexes. At higher temperatures, larger particles of the system grow at the expense of the smaller ones in the spirit of Ostwald ripening, and the correlation functions are described by a single stretched exponential with values of β suggesting a collection of species with narrow size distributions at high temperatures. The size of the unimers ($R_{h,f} \leq 2$ nm) increases with the PNIPAAM block length, and the temperature-induced growth of the interchain structures is stronger when the length of the PNIPAAM block increases. (iv) By adding salt, the unimers/micelles ($R_{h,f} \leq 4$ nm) grow, but only slight temperature dependence of $R_{h,f}$ was observed in the considered temperature range. The size ($R_{h,s}$) of the intermicellar complexes is strongly compressed at low temperatures upon salt addition because of screening of Coulomb repulsions. At high temperatures, the temperature-induced growth is modest at low levels of salt addition and it becomes significantly stronger at high salt concentration. The rise of $R_{h,s}$ is also strong in the absence of salt, and it seems that a small amount of added salt promotes stabilization of the species as the temperature increases.

AUTHOR INFORMATION

Present Address

[§]Division of Physical Chemistry, Department of Chemistry, Center for Chemistry and Chemical Engineering, Lund University, P.O. Box 124, SE-221 00 Lund, Sweden.

Notes

The authors declare no competing financial interest.

ACKNOWLEDGMENTS

The financial support of the Norwegian Research Council through the project 177665/V30 is gratefully acknowledged.

REFERENCES

(1) Muthukumar, M.; Ober, C. K.; Thomas, E. L. *Science* **1997**, *277*, 1225.
(2) Förster, S.; Antonietti, M. *Adv. Mater.* **1998**, *10*, 195.
(3) Kjøniksen, A.-L.; Laukkanen, A.; Galant, C.; Knudsen, K. D.; Tenhu, H.; Nyström, B. *Macromolecules* **2005**, *38*, 948.
(4) *Responsive Polymer Materials: Design and Applications*; Minko, S., Ed.; Blackwell Publishing: Ames, IA, 2006.
(5) *Block Copolymers in Nanoscience*; Lazzari, M., Liu, G., Lecommandoux, S., Eds. ; Wiley-VCH: Weinheim, Germany, 2006.
(6) Zhu, K.; Jin, H.; Kjøniksen, A.-L.; Nyström, B. *J. Phys. Chem. B* **2007**, *111*, 10862.
(7) Zhu, K.; Pamies, R.; Kjøniksen, A.-L.; Nyström, B. *Langmuir* **2008**, *24*, 14227.
(8) Bertrand, N.; Fleischer, J. G.; Wasan, K. M.; Leroux, J.-C. *Biomaterials* **2009**, *30*, 2598.
(9) Wei, H.; Cheng, S.-X.; Zhang, X.-Z.; Zhuo, R.-X. *Prog. Polym. Sci.* **2009**, *34*, 893.
(10) Kjøniksen, A.-L.; Zhu, K.; Behrens, M. A.; Pedersen, J. S.; Nyström, B. *J. Phys. Chem. B* **2011**, *115*, 2125.
(11) Zhang, X. Z.; Zhuo, R. X. *Mater. Lett.* **2002**, *52*, 5.
(12) Jones, C. D.; Lyon, L. A. *Macromolecules* **2003**, *36*, 1988.
(13) Kjøniksen, A.-L.; Nyström, B.; Tenhu, H. *Colloids Surf., A* **2003**, *228*, 75.
(14) Chaw, C. S.; Chooi, K. W.; Liu, X. M.; Tan, C. W.; Wang, L.; Yang, Y. Y. *Biomaterials* **2004**, *25*, 4297.
(15) Gao, C.; Möhwald, H.; Shen, J. *Polymer* **2005**, *46*, 4088.
(16) Morishima, Y. *Angew. Chem., Int. Ed.* **2007**, *46*, 1370.
(17) Schild, H. G. *Prog. Polym. Sci.* **1992**, *17*, 163.
(18) Kvon, G. S.; Kataoka, K. *Adv. Drug. Delivery Rev.* **1995**, *16*, 295.
(19) Kjøniksen, A.-L.; Zhu, K.; Pamies, R.; Nyström, B. *J. Phys. Chem. B* **2008**, *112*, 3294.
(20) Wang, J. S.; Matyjaszewski, K. *J. Am. Chem. Soc.* **1995**, *117*, 5614.
(21) Matyjaszewski, K.; Xia, J. *Chem. Rev.* **2001**, *101*, 2921.
(22) Dedinaite, A.; Thormann, E.; Olanya, G.; Claesson, P. M.; Nyström, B.; Kjøniksen, A.-L.; Zhu, K. *Soft Matter* **2010**, *6*, 2489.
(23) Pamies, R.; Zhu, K.; Volden, S.; Kjøniksen, A.-L.; Karlsson, G.; Glomm, W. R.; Nyström, B. *J. Phys. Chem. C* **2010**, *114*, 21960.

(24) Lazzara, G.; Olofsson, G.; Alfredsson, V.; Zhu, K.; Nyström, B.; Schillén, K. *Soft Matter* **2012**, *8*, 5043.
(25) Behrens, M. A.; Lopez, M.; Kjøniksen, A.-L.; Zhu, K.; Nyström, B.; Pedersen, J. S. *Langmuir* **2012**, *28*, 1105.
(26) Pamies, R.; Zhu, K.; Kjøniksen, A.-L.; Nyström, B. *Polym. Bull.* **2009**, *62*, 487−502.
(27) Xia, Y.; Burke, N. A. D.; Stöver, H. D. H. *Macromolecules* **2006**, *39*, 2275.
(28) Siegert, A. J. F. Massachusetts Institute of Technology, Radiation Laboratory Report No. 465, 1943.
(29) Chen, H.; Ye, X.; Zhang, G.; Zhang, Q. *Polymer* **2006**, *47*, 8367.
(30) Maleki, A.; Kjøniksen, A.-L.; Zhu, K.; Nyström, B. *J. Phys. Chem. B* **2011**, *115*, 8975.
(31) Rodriguez-Hernández, J.; Chécot, F.; Gnanou, Y.; Lecommandoux, S. *Prog. Polym. Sci.* **2005**, *30*, 691.
(32) Malcolm, G. N.; Rowlinson, J. S. *Trans. Faraday Soc.* **1957**, *53*, 921.
(33) Chen, J.; Liu, M.; Gong, H.; Huang, Y.; Chen, C. *J. Phys. Chem. B* **2011**, *115*, 14947.
(34) Baulin, V. A.; Halperin, A. *Macromolecules* **2002**, *35*, 6432.
(35) Karlström, G. *J. Phys. Chem.* **1985**, *89*, 4962.
(36) Matsuyama, A.; Tanaka, F. *Phys. Rev. Lett.* **1990**, *65*, 341.
(37) De Gennes, P.-G. *C. R. Acad. Sci., Ser. II* **1991**, *313*, 1415.
(38) Painter, P. C.; Berg, L. P.; Veytsman, B.; Coleman, M. M. *Macromolecules* **1997**, *30*, 7529.
(39) Borisov, O. V.; Halperin, A. *Macromolecules* **1999**, *32*, 5097.
(40) Pelton, R. *J. Colloid Interface Sci.* **2010**, *348*, 673.
(41) Alaghemandi, M.; Spohr, E. *Macromol. Theory Simul.* **2012**, *21*, 106.
(42) Schmidt, R. R.; Pamies, R.; Kjøniksen, A.-L.; Zhu, K.; Cifre, J. G. H.; Nyström, B.; de la Torre, J. G. *J. Phys. Chem. B* **2010**, *114*, 8887.
(43) Lechner, M. D. *J. Serb. Chem. Soc.* **2005**, *70*, 361.
(44) Al-Manasir, N.; Zhu, K.; Kjøniksen, A.-L.; Knudsen, K. D.; Karlsson, G.; Nyström, B. *J. Phys. Chem. B* **2009**, *113*, 11115.
(45) Ostwald, W. *Analytische Chemie*, 3rd ed.; Engelmann: Leipzig, Germany, 1901; p 23.
(46) Lifshitz, I. M.; Slyozov, V. V. *J. Phys. Chem. Solids* **1961**, *19*, 35.
(47) Wagner, C. *Z. Elektrochem.* **1961**, *65*, 581.
(48) Voorhees, P. W. *J. Stat. Phys.* **1985**, *38*, 231.
(49) Madras, G.; McCoy, B. J. *J. Chem. Phys.* **2001**, *115*, 6699.
(50) Liu, Y.; Kathan, K.; Saad, W.; Prud'homme, R. K. *Phys. Rev. Lett.* **2007**, *98*, 036102.
(51) Madras, G.; McCoy, B. J. *Chem. Eng. Sci.* **2002**, *57*, 3809.
(52) Talapin, D. V.; Rogach, A. I.; Haase, H.; Weller, H. *J. Phys. Chem. B* **2001**, *105*, 12278.
(53) Behrens, M. A.; Kjøniksen, A.-L.; Zhu, K.; Nyström, B.; Pedersen, J. S. *Macromolecules* **2012**, *45*, 246.
(54) Förster, S.; Schmidt, M.; Antonietti, M. *Polymer* **1990**, *31*, 781.
(55) Dobrynin, A. V. *Curr. Opin. Colloid Interface Sci.* **2008**, *13*, 376.
(56) Shusharina, N. P.; Rubinstein, M. In *Nanostructured Soft Matter − Experiment, Theory, Simulation, and Perspectives*; Zvelindovsky, A. V., Ed.; Canopus Publishing Limeted: Bristol, U.K., 2007; pp 301−326.
(57) Gohy, J.-F.; Lohmeijer, B. G. G.; Varshney, S. K.; Schubert, U. S. *Macromolecules* **2002**, *35*, 7427.